Hindawi Publishing Corporation
Advances in Optical Technologies
Volume 2012, Article ID 484235, 7 pages
doi:10.1155/2012/484235

Research Article

Laser Performance of 1% at. Yb : Lu_2O_3 Ceramic

Angela Pirri, Guido Toci, and Matteo Vannini

Istituto di Fisica Applicata "N. Carrara"(IFAC), Consiglio Nazionale delle Ricerche (CNR), Via Madonna del Piano 10 C, Sesto Fiorentino, 50019 Florence, Italy

Correspondence should be addressed to Guido Toci, g.toci@ifac.cnr.it

Received 9 December 2011; Accepted 31 January 2012

Academic Editor: Richard C. Powell

We present the performance of a laser prototype based on 1% at. Yb : Lu_2O_3 ceramic, longitudinally pumped in quasi-CW regime at 968 nm. A slope efficiency of 49% with respect to the absorbed pump power was obtained for laser operation at 1032.5 nm. We studied the effects on the laser oscillation due to the reinjection of the residual pump. The thermal behavior of the sample was investigated by means of numerical simulations, accounting for the different thermal load resulting from spontaneous and laser emission. Finally, we report the measured level of the Amplified Spontaneous Emission, which is found to be less than 0.1 mW.

1. Introduction

Since their appearance on the scene, polycrystalline transparent materials of cubic structure doped [1–4] with rare earths as Nd^{3+} [5–7] and Yb^{3+} [8–10], are found to be appealing as laser gain materials showing all their potentiality in term of shortness of the pulse [11–13], average power level and beam quality. In consequence of that, in the past years many efforts have been made to improve and refine the techniques of fabrication paving the way to a new class of diode-pumped solid-state lasers. In fact, the excellent goals achieved in different host materials [14–19] testify that lasers based on ceramic materials exhibit performances comparable with the corresponding single crystals.

The reasons underlying these successful results are multiple and closely related to both the optical and the physical properties of the host ceramics. The host material plays a crucial role to reach an efficient laser action. In fact, it modifies the intrinsic properties of doping ions as the lifetime of the states involved in the laser action as well as the Stark level structure and the absorption and emission cross-sections. Moreover, it determines by its own thermal properties the thermal dissipation of the whole gain medium, and then the magnitude of the thermal gradients due to the pumping process, which induces stress and strain inside the lasing sample determining a modification of the refractive index. The undesirable consequences are the depolarization and degradation of the laser beam quality, the change of the resonator stability condition, and an increase of losses. It has been demonstrated that ceramics show better thermomechanical properties [20, 21]; indeed, they withstand higher thermo-mechanical stresses with respect to the crystals. The lower temperatures of sintering have allowed, for instance, the growth of good optical quality sesquioxides as Y_2O_3, Sc_2O_3 and Lu_2O_3, which are very hard to grow as single crystals because of their high melting points (above 2400°C), which does not allow the use of conventional methods as the Czochralski process but rather sophisticate technique as the heat exchanger or Bridgman methods [22]. Moreover, ceramics can sustain high levels of doping with a uniform dopant distribution preserving a good optical quality (Yb : YAG samples with concentration higher than 15% are commercially available). Finally, they can be easily codoped or fabricated with a gradient of concentration, which permits a more uniform distribution of the heat load during the pumping process.

To focus on Lu_2O_3 [23], this is quite interesting for two main reasons. First, it has a high undoped thermal conductivity, (i.e., $K = 12.2$ W/mK measured at 50°C, according to Griebner et al. [24], $K = 14.3$ W/mK at room temperature according to Novoselov et al. [25]). Secondly, its thermal conductivity is only slightly affected by the level of doping. In

general, K decreases when the lattice is doped because of the different atomic weight of dopand ion and the substituted host cation. The phonons, which are mainly responsible in Lu_2O_3 of the heat transportation, are basically scattered at the mass defect with the consequence of an unavoidable reduction of the thermal conductivity, which is further enhanced by increasing the concentration of dopants. In the case of 2.7% at. $Yb:Lu_2O_3$ crystal the thermal conductivity was measured finding a slight reduction to 10.8 W/mK because Yb^{3+} has an atomic weight quite similar to Lu^{3+}.

Among the rare earths, in the last decade the research has been focused on Yb ion because it has a simple electronic energy scheme consisting of only two manifolds, that is, $^2F_{5/2}$ and $^2F_{7/2}$. The relatively small quantum defect results in a small fraction of pump power deposited as heat in the gain medium, which permits the use of Yb in those applications were high-intense pump power is required. Due to the high absorption cross section centered at around 978 nm (almost close to the zero line), Yb can be efficiently pumped by commercial diode lasers, while its broad emission band permits a wide range of tunability and generates pulses with a short duration in various operation regimes. Finally, Yb ion is less prone to show parasitic decay paths that deplete the population of the upper state of the laser transition such as nonradiative decay paths or upconversion processes.

Basically, to obtain good laser performances gain media with appropriate level of doping are carefully chosen (generally above 3% at.). However, samples activated with low concentration of dopants are strategic in the totality of amplifier systems because the amplification of high energy pulses has to be reached avoiding the amplification of the spontaneous emission.

This paper reports the laser performance achieved by a prototype of laser based on low-doped 1% at. $Yb:Lu_2O_3$ ceramic. The sample is longitudinally pumped with two different schemes, that is, with and without the reinjection of the residual pump emerging from the lasing medium, at 968 nm in quasi-Continuous Wave. A comparison of data obtained in both pumping schemes allowed us to study the effect of the recycled pump beam on the laser performance. Good results are achieved with both pumping schemes either when the sample emits at 1032 nm or at 1078 nm. In particular, the maximum output power is measured when the reinjection of the residual pump is active, that is, 1.8 W at 1032 nm. Conversely, the highest slope efficiency of 49% is obtained at the same laser wavelength when the residual pump is switched off.

The thermal behavior of the sample is studied by calculating the expected temperature distribution with numerical simulations, which show the impact of the pump beam reinjection and the lasing wavelength on the sample. Finally, we measured the level of the ASE.

2. Experimental Setup

The V-shaped laser cavity is schematically shown in Figure 1. The pump source is a laser-diode delivering up to 20 W at 968 nm coupled to a 100 μm fibre with numerical aperture

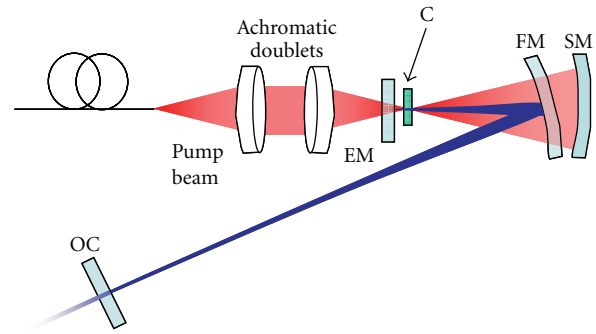

Figure 1: Laser cavity. EM: end-mirror (flat); FM: folding mirror (ROC 100 mm); SM: spherical mirror; OC: output coupler (flat); C: denotes the gain material.

of 0.15. The intensity distribution of the pump in the focal plane is almost Gaussian with a spot radius of 67 μm at $1/e^2$. The sample, which was grown by Baikowski Japan Co. Ltd, is pumped in quasi-Continuous Wave (Duty Factor of 20%) with the repetition rate of 10 Hz, through the cavity End-Mirror (EM) by a pair of achromatic doublets with a magnification of 1 : 1. EM is a flat mirror with a dichroic coating with high transmission around the pump wavelength and high reflectivity for wavelengths longer than 1000 nm. The A/R coated ceramic sample has a doping level of 1% at. with a thickness of 3 mm. It is soldered with Indium on a copper heat sink, which is water-cooled at 18°C.

The Folding-Mirror (FM) has a curvature radius of 100 mm, and it features a high transmission at 968 nm. The Spherical Mirror (SM) placed in the rear side of the FM, concentric with respect to the focus of the pump beam, is used to collect and reinject into the sample the residual pump beam passing through the FM. This increases the overall absorption of the incident pump power by about 7.9%. The absorption of the pump power when the SM is blocked is measured to be 18.2%. Although the absorption cross sections at 968 nm is low, that is, σ_{abs} (968 nm) = 0.27×10^{-20} cm^2, it is relatively insensitive to the variation of the pump wavelength, which is kept constant at the different pumping powers by changing the cooling temperature of the laserdiode. This arrangement reduces the requirement of a tight stabilization of the pump emission wavelength over a wide range of laser-diode input, as required by the narrow width of the absorption peak (3 nm FWHM in Lu_2O_3 [11]) and the pump beam (above 5 nm FWHM).

3. Results and Discussion

We measured the output power as a function of the absorbed pump power by four OC mirrors with different transmittance, that is, $T = 2.1\%$, $T = 5.5\%$, $T = 6.7\%$, and $T = 11.8\%$. Moreover, two different pumping configurations are employed, that is, with and without the recycling of the pump radiation coming out from the sample. In the former configuration (hereon named single pass) the pump radiation reflected by the SM is blocked while in the latter scheme (namely, double pass) the sample is longitudinally

pumped also from the rear surface by the SM. A comparison of the two sets of data allowed us to study the effect of the recycled pump on the gain sample.

Some general considerations can be carried out from the results concerning the wavelength of the laser emission, the slope efficiency and the maximum output power.

To focus on the emission laser wavelength, the sample is able to emit at 1032.5 nm and 1078 nm, which corresponds to the transition between the lower energetic state of the $^2F_{5/2}$ and the two higher energetic sublevels of the $^2F_{7/2}$, respectively. As clearly shown in Figure 2, this does not depend on the pumping scheme but it is basically connected to the transmittance of the OC coupling mirror and to the reabsorption of the sample at the mentioned wavelengths. Mirrors with low transmission require a smaller fraction of inverted population to achieve the laser threshold, determining a shift in the peak of the actual gain spectrum toward longer wavelengths. Moreover, the reabsorption at around 1078 nm is smaller than at shorter wavelength due to the higher overlapping between the absorption and the emission regions. Figure 2(a) shows the performance achieved by employing an OC with a transmission of $T = 2.1\%$. Output coupler mirrors with higher transmittances, from 5.5% to 11.8%, push the laser emission at 1032.5 nm as shown in Figures 2(b), 2(c), and 2(d) and allow reaching higher laser output power. In particular, we measured the maximum output power of 1.8 W with $T = 11.8\%$ when the residual pump radiation is recycled, Figure 2(d).

Concerning the output powers and the corresponding slope efficiencies, the results show a net dependence on the pumping scheme. For instance, with $T = 2.1\%$, in double pass, we measured an output power of 1.5 W with a corresponding slope efficiency 34% and a threshold of 0.65 W. In single pass, we observed a decrease of around 27% of the output power, 1.2 W, and an increase of around 6% of the slope efficiency, that is, $\eta = 39\%$. The threshold is slightly increased, 0.72 W. Similar results are found with the other output couplers. With $T = 11.8\%$, in double pass, the slope efficiency is estimated to be $\eta = 45\%$ while it increases to 48% when the SM action is avoided. Conversely, it causes a decrease of around 35% of the output power, from 1.8 W to 1.3 W. In all cases, the slope efficiency is estimated taking into account all points for each curve. The deviation of the output power from the theoretically expected straight line is easily explained by the progressive saturation of the reabsorption in the peripheral regions of the laser mode [26].

The enhancement of the output power observed when the residual pump is recycled is addressed to the enhancement of the absorption at 968 nm from the medium. As reported above it increases from 18.2% (single pass) to 24% (double pass). However, the optical quality of the reinjected pump radiation is degraded due to several reasons, for instance: the thermal lensing in the sample, the saturation of the absorption on the beam axis, and the astigmatism introduced by the tilted spherical surfaces of the FM. Therefore, the size of the reinjected focal spot is slightly larger than that of the first pass, resulting in a lower efficiency for the contribution of the reinjected pump with respect to the overall laser output.

4. Thermal Simulations

As stated above, Lu_2O_3 is an attractive host for high power laser application because of its high thermal conductivity which, in case of Yb doping, is only slightly sensitive to the doping level.

In order to get insights on the thermal behavior of the sample under test, we carried out a numerical simulation to calculate the temperature distribution in the ceramic by Finite Element Analysis (FEM), using the Partial Differential Equation Toolbox implemented in MATLAB.

In particular we considered a sample with cylindrical symmetry, with radius of 2.5 mm and length 3 mm. The pump and the laser beam propagate along the symmetry axis. The pump beam has a Gaussian profile, with radius in the waist $w_P = 67\,\mu$m and $Z_R = 0.87$ mm in the material. These values correspond to the actual parameters of the pump beam in our experimental set up, as resulting from the measurements carried out with a CCD camera for laser beam diagnostics.

The focus of the pump beam is set in the center of the sample. The laser beam was assumed to be Gaussian, with radius 60 μm @ $1/e^2$ and negligible diffraction along the sample length. The sample is in contact with the heat sink at 291 K on a ring with $1.0\,\text{mm} < r < 2.5\,\text{mm}$ on the opposite side with respect to the incoming pump beam; the thermal resistance of the Indium layer used for the welding was accounted for (heat transfer coefficient 9×10^3 W/(m^{2}K) [26]). A small cooling due to natural air convection is assumed to occur on the other sample sides (heat transfer coefficient 10 W/(m^{2}K) [27]).

The absorbed power density is calculated assuming an exponential absorption of the pump beam in the sample, with an absorption length α equal to the value with unsaturated absorption. This is a reasonable approximation when in lasing condition, because it results both from rate equation models and from experimental measurements on several Yb-doped materials [28–30] that the fast deexcitation of the upper level due to the laser beam counteracts the saturation of the absorption at the pump wavelength. The resulting expression is

$$\begin{aligned} W_{\text{abs}}(r,z) &= \alpha I_P(r,z) \\ &= \alpha\left(\frac{2P_p}{\pi w_p^2\left(1+\left(z-z_f\right)/z_R\right)}\right) \\ &\quad\times \exp\left[\frac{-2r^2}{w_p^2\left(1+\left(z-z_f\right)/z_R\right)}\right] \\ &\quad\times \left\{e^{-\alpha z}+\rho\left(1-e^{-\alpha L}\right)e^{-\alpha(L-z)}\right\}. \end{aligned} \tag{1}$$

The term in curly brackets accounts for the contribution of the first pass and second pass pump beam. The reinjection efficiency of the pump beam is accounted for by the coefficient ρ. In the simulations we assumed $\rho = 0.77$, accounting

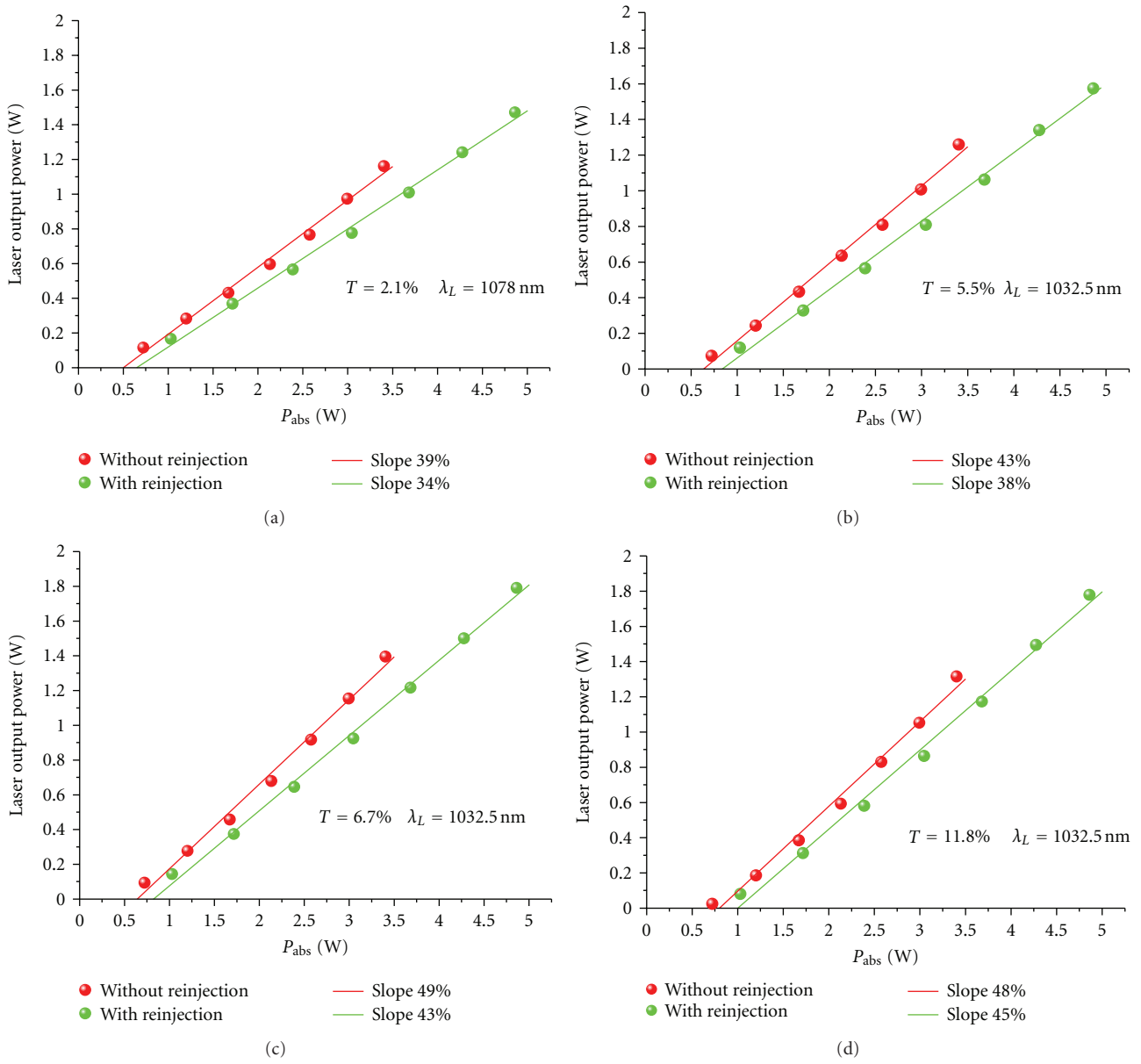

Figure 2: Laser output power versus the absorbed pump power with and without the recycled pump radiation. The maximum input pump power is 18.7 W at 968 nm corresponding to 4.86 W (with reinjection) and 3.4 W (without reinjection) of the absorbed pump power.

for the double pass Fresnel losses on the crystal surface (transmission 0.902) and 5% losses on the other optics. The local power dissipation in the sample depends on the local balance between spontaneous decay rate (which is assumed to occur at a wavelength $\lambda_F = 1015.6$ nm, corresponding to the average of the fluorescence band, as calculated from the data reported in [11]) and the stimulated emission at the laser wavelength λ_L (see for instance Chénais et al. [28]). In absence of other decay processes, the dissipated power distribution is then given by

$$W_{\text{dis}}(r,z) = W_{\text{abs}}(r,z)\left[1 - \frac{\lambda_P}{\lambda_F}\frac{1}{1+R(r,z)} - \frac{\lambda_P}{\lambda_L}\frac{R(r,z)}{1+R(r,z)}\right], \tag{2}$$

where $R(r,z)$ is the ratio between the stimulated and the spontaneous decay rate, given by

$$R(r,z) = \lambda_L \tau\left[\sigma_e(\lambda_L) - \sigma_a(\lambda_L)\left(\frac{N_1(r,z)}{N_2(r,z)}\right)\right]\frac{I_L(r,z)}{hc}, \tag{3}$$

where N_1 and N_2 are the population in the upper and lower laser level, $\sigma_{e,a}(\lambda_L)$ are the emission and absorption cross sections at λ_L, I_L is the laser intensity, τ is the upper level lifetime. The ratio between N_1 and N_2 is given by

$$\frac{N_1(r,z)}{N_2(r,z)} = \frac{(\lambda_L I_L(r,z)\sigma_e(\lambda_L) + \lambda_P I_P(r,z)\sigma_e(\lambda_P) + (hc/\tau))}{(\lambda_L I_L(r,z)\sigma_a(\lambda_L) + \lambda_P I_P(r,z)\sigma_a(\lambda_P))}. \tag{4}$$

Table 1: Thermal and spectroscopic parameters used in the simulations. The value of the thermal conductivity is interpolated from the measurements reported in [25].

Parameter	Value	Reference
Thermal cond. (W/(mK))	13.23	[25]
Spec. heat (J/(m^3 K))	2.69×10^6	[31]
σ_e(968 nm) (m^2)	0.175×10^{-24}	[11]
σ_e(1032.5 nm) (m^2)	1.044×10^{-24}	[11]
σ_e(1078 nm) (m^2)	0.30×10^{-24}	[11]
σ_a(968 nm) (m^2)	0.31×10^{-24}	[11]
σ_a(1032.5 nm) (m^2)	0.13×10^{-24}	[11]
σ_a(1078 nm) (m^2)	0.006×10^{-24}	[11]
Absorption const. α (m^{-1})	67	—
Decay time τ (ms)	0.805	[32]

In this model, the intracavity circulating laser intensity I_L is determined from the experimental value of the output power as reported in Figure 2. QCW pumping dynamics at 10 Hz of repetition rate, 20% duty factor, was also implemented in the model. The parameters used in the simulation are resumed in the Table 1.

Figure 3 shows the calculated temperature distribution at the end of the 50th pump pulse, with pump reinjection and laser oscillation occurring at 1032.5 nm. It can be seen that the temperature increase with respect to the heat sink is moderate, that is, only 3.5 K. The temperature peak is located in correspondence of the pump beam focus. The reinjection of the residual pump determines only a slight increase in the temperature with respect to the configuration without pump reinjection. This can be seen by comparing Figures 3 and 4, where the simulation is carried out for the configuration without pump reinjection. The peak temperature results are about 0.7 K lower than in the case of pump reinjection. It can be also noticed that the temperature profile is less symmetrical with respect to the focal plane of the pump beam.

The value of the lasing wavelength and of the intracavity circulating power can greatly affect the thermal load in the sample, and then the temperature distribution. In particular, an increase in the intracavity circulating power results in an increased stimulated decay rate with respect to spontaneous emission (see (3)). When the lasing wavelength λ_L is larger than the average fluorescence wavelength λ_F (so that the average energy defect between pump and emitted photon is larger for laser photons than for fluorescence photons) this results in an increased thermal load. The thermal load also increases when the lasing wavelength is moved toward longer wavelengths, because this increases the energy defect between pump and laser photon.

Both the effects described above occur when the sample operates with the output coupler having $T = 2.1\%$ (see Figure 2), which for a given pump power increases the intracavity circulating power and it pushes the emission wavelength to 1078 nm. The calculated temperature distribution for the maximum pump power is shown in Figure 5. It appears that the peak temperature value is much higher than in the case of Figure 3 (same pump power, but lasing at 1032.5 nm with output coupler transmission $T = 11.8\%$).

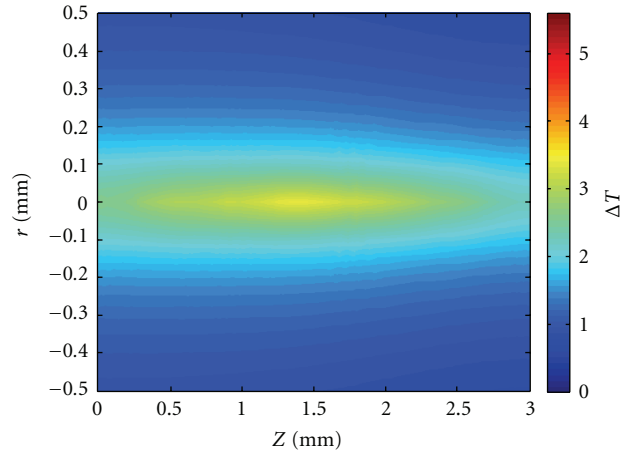

Figure 3: Simulated temperature distribution after 50 pump pulses. Peak incident pump power 18.7 W, output peak power 1.8 W, $T = 11.8\%$, emission wavelength 1032.5 nm. The heat sink and the pump injection side are at $Z = 0$ mm. Pump reinjection is implemented (reinjection efficiency $\rho = 0.77$). The value of the temperature is the difference with respect to the heat sink.

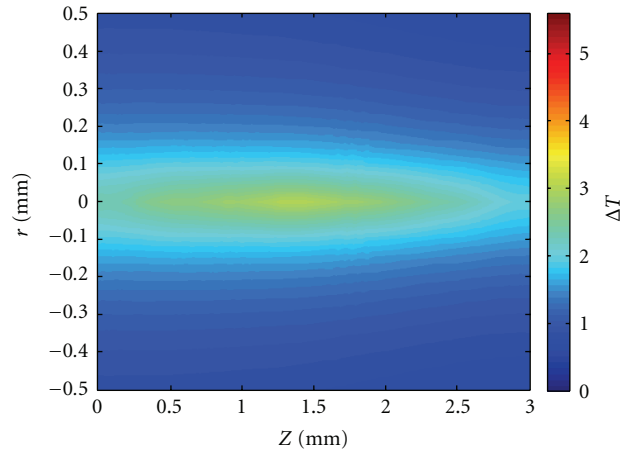

Figure 4: Simulated temperature distribution after 50 pump pulses. Peak incident pump power 18.7 W, output peak power 1.8 W, $T = 11.8\%$, and emission wavelength 1032.5 nm. The heat sink and the pup injection side are at $Z = 0$ mm. Pump reinjection is suppressed (reinjection efficiency $\rho = 0$). The value of the temperature is the difference with respect to the heat sink.

5. Conclusions

In this paper we have described the laser oscillation achieved on Yb-doped Lu_2O_3 ceramic with a doping level of 1% at. in quasi-CW pumping with a laser diode emitting at 968 nm. We investigated its performances in two different pumping configurations, that is, with and without the reinjection of the residual pump coming out from the sample. Moreover, we measured the levels of Amplified Spontaneous Emission

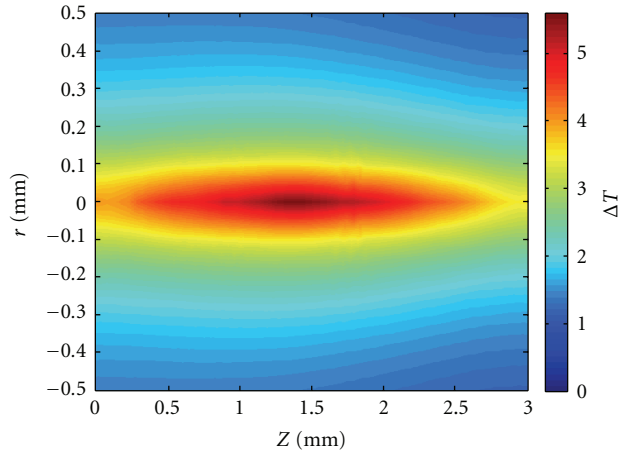

Figure 5: Simulated temperature distribution after 50 pump pulses. Peak incident pump power 18.7 W, output peak power 1.5 W, $T = 2.1\%$, and emission wavelength 1078 nm. The heat sink and the pup injection side are at $Z = 0$ mm. Pump reinjection is implemented (reinjection efficiency $\rho = 0.77$). The value of the temperature is the difference with respect to the heat sink.

present in the ceramic. The good results achieved in terms of output power, slope efficiency, and threshold of the laser action, suggest that Yb : Lu_2O_3 is an excellent laser medium and, at the same time, low-doped Lu_2O_3 ceramic can be useful for high energy amplification of broadband signals. Finally, we have studied the thermal behavior of the sample with numerical simulations accounting for the pump beam and the laser action. According to the theoretical expectation, in double pass pumping scheme the sample undergoes a more severe temperature increase, which can contribute to the observed reduction of the laser efficiency with respect to the single pass pumping configuration.

Acknowledgments

This research was supported by Regione Toscana, project *CTOTUS—Progetto integrato per lo sviluppo della Capacità Tecnologica e Operativa della Toscana per l'Utilizzo dello Spazio* (Programma Operativo Regionale, Fondo Europeo di Sviluppo Regionale 2007–2013 Attività 1.1 Linea d'intervento D) and by the Consiglio Nazionale delle Ricerche *Ricerca Spontanea a Tema Libero* (CNR-RSTL), id. 959.

References

[1] K. Takaichi, H. Yagi, J. Lu et al., "Yb^{3+}-doped $Y_3Al_5O_{12}$ ceramics—a new solid-state laser material," *Physica Status Solidi (A) Applied Research*, vol. 200, no. 1, pp. R5–R7, 2003.

[2] J. Lu, K. Takaichi, T. Uematsu et al., "Yb^{3+}: Y_2O_3 ceramics—a novel solid-state laser material," *Japanese Journal of Applied Physics*, vol. 41, no. 12 A, pp. L1373–L1375, 2002.

[3] K. Takaichi, H. Yagi, A. Shirakawa et al., "Lu_2O_3: Yb^{3+} ceramics—a novel gain material for high-power solid-state lasers," *Physica Status Solidi (A) Applications and Materials*, vol. 202, no. 1, pp. R1–R3, 2005.

[4] A. Ikesue and Y. L. Aung, "Ceramic laser materials," *Nature Photonics*, vol. 2, no. 12, pp. 721–727, 2008.

[5] A. Ikesue, T. Kinoshita, K. Kamata, and K. Yoshida, "Fabrication and optical properties of high-performance polycrystalline Nd:YAG ceramics for solid-state lasers," *Journal of the American Ceramic Society*, vol. 78, no. 4, pp. 1033–1040, 1995.

[6] J. Lu, K. Takaichi, T. Uematsu et al., "Promising ceramic laser material: highly transparent Nd^{3+}: Lu_2O_3 ceramic," *Applied Physics Letters*, vol. 81, no. 23, pp. 4324–4326, 2002.

[7] V. Lupei, A. Lupei, and A. Ikesue, "Transparent Nd and (Nd, Yb)-doped Sc_2O_3 ceramics as potential new laser materials," *Applied Physics Letters*, vol. 86, no. 11, Article ID 111118, pp. 1–3, 2005.

[8] A. A. Kaminskii, S. N. Bagayev, K. Ueda et al., "New results on characterization of highly transparent C-modification Lu_2O_3 nanocrystalline ceramics: room-temperature tunable CW laser action of Yb^{3+} ions under LD-pumping and the propagation kinetics of non-equilibrium acoustic phonons," *Laser Physics Letters*, vol. 3, no. 8, pp. 375–379, 2006.

[9] K. Takaichi, H. Yagi, P. Becker et al., "New data on investigation of novel laser ceramic on the base of cubic scandium sesquioxide: two-band tunable CW generation of Yb^{3+} :Sc_2O_3 with laser-diode pumping and the dispersion of refractive index in the visible and near-IR of undoped Sc_2O_3," *Laser Physics Letters*, vol. 4, no. 7, pp. 507–510, 2007.

[10] A. Pirri, D. Alderighi, G. Toci, and M. Vannini, "High-efficiency, high-power and low threshold Yb^{3+}:YAG ceramic laser," *Optics Express*, vol. 17, no. 25, pp. 23344–23349, 2009.

[11] M. Tokurakawa, K. Takaichi, A. Shirakawa et al., "Diode-pumped mode-locked Yb^{3+}:Lu_2O_3 ceramic laser," *Optics Express*, vol. 14, no. 26, pp. 12832–12838, 2006.

[12] J. Dong, K. I. Ueda, A. Shirakawa, H. Tagi, T. Yanagitani, and A. A. Kaminskii, "Composite Yb:YAG/Cr^{4+}:YAG ceramics picosecond microchip lasers," *Optics Express*, vol. 15, no. 22, pp. 14516–14523, 2007.

[13] H. Yoshioka, S. Nakamura, T. Ogawa, and S. Wada, "Diode-pumped mode-locked Yb: YAG ceramic laser," *Optics Express*, vol. 17, no. 11, pp. 8919–8925, 2009.

[14] J. Kong, D. Y. Tang, B. Zhao et al., "9.2-W diode-end-pumped Yb: Y_2O_3 ceramic laser," *Applied Physics Letters*, vol. 86, no. 16, Article ID 161116, pp. 1–3, 2005.

[15] S. Nakamura, H. Yoshioka, Y. Matsubara, T. Ogawa, and S. Wada, "Broadly Tunable Yb^{3+}-Doped $Y_3Al_5O_{12}$ ceramic laser at room temperature," *Japanese Journal of Applied Physics*, vol. 48, no. 6, Article ID 060205, 2009.

[16] J. Kong, D. Y. Tang, C. C. Chan et al., "High-efficiency 1040 and 1078 nm laser emission of a Yb: Y_2O_3 ceramic laser with 976 nm diode pumping," *Optics Letters*, vol. 32, no. 3, pp. 247–249, 2007.

[17] M. Tokurakawa, A. Shirakawa, K. I. Ueda et al., "Diode-pumped 65 fs Kerr-lens mode-locked Yb^{3+}: Lu_2O_3 and non-doped Y_2O_3 combined ceramic laser," *Optics Letters*, vol. 33, no. 12, pp. 1380–1382, 2008.

[18] A. Pirri, G. Toci, D. Alderighi, and M. Vannini, "Effects of the excitation density on the laser output of two differently doped Yb:YAG ceramics," *Optics Express*, vol. 18, no. 16, pp. 17262–17272, 2010.

[19] J. Sanghera, J. Frantz, W. Kim et al., "10% Yb^{3+}-Lu_2O_3 ceramic laser with 74% efficiency," *Optics Letters*, vol. 36, no. 4, pp. 576–578, 2011.

[20] A. A. Kaminskii, M. Sh. Akchurin, R. V. Gainutdinov et al., "Microhardness and fracture toughness of Y_2O_3- and $Y_3Al_5O_{12}$-based nanocrystalline laser ceramics," *Crystallography Reports*, vol. 50, no. 5, pp. 869–873, 2005.

[21] A. A. Kaminskii, M. S. Akchurin, P. Becker et al., "Mechanical and optical properties of Lu_2O_3 host-ceramics for Ln^{3+} lasants," *Laser Physics Letters*, vol. 5, no. 4, pp. 300–303, 2008.

[22] V. Peters, A. Bolz, K. Petermann, and G. Huber, "Growth of high-melting sesquioxides by the heat exchanger method," *Journal of Crystal Growth*, vol. 237-239, no. 1–4, pp. 879–883, 2002.

[23] A. Pirri, G. Toci, and M. Vannini, "First laser oscillation and broad tunability of 1 *at.* % Yb-doped Sc_2O_3 and Lu_2O_3 ceramics," *Optics Letters*, vol. 36, no. 21, pp. 4284–4286, 2011.

[24] U. Griebner, V. Petrov, K. Petermann, and V. Peters, "Passively mode-locked Yb:Lu_2O_3 laser," *Optics Express*, vol. 12, no. 14, pp. 3125–3130, 2004.

[25] A. Novoselov, J. H. Mun, R. Simura, A. Yoshikawa, and T. Fukuda, "Micro-pulling-down: a viable approach to the crystal growth of refractory rare-earth sesquioxides," *Inorganic Materials*, vol. 43, no. 7, pp. 729–734, 2007.

[26] T. Taira, W. M. Tulloch, and R. L. Byer, "Modeling of quasi-three-level lasers and operation of cw Yb:YAG lasers," *Applied Optics*, vol. 36, no. 9, pp. 1867–1874, 1997.

[27] A. K. Cousins, "Temperature and thermal stress scaling in finite-length end-pumped laser rods," *IEEE Journal of Quantum Electronics*, vol. 28, no. 4, pp. 1057–1069, 1992.

[28] S. Chénais, F. Druon, S. Forget, F. Balembois, and P. Georges, "On thermal effects in solid-state lasers: the case of ytterbium-doped materials," *Progress in Quantum Electronics*, vol. 30, no. 4, pp. 89–153, 2006.

[29] A. Pirri, D. Alderighi, G. Toci, M. Vannini, M. Niki, and H. Sato, "Direct Comparison of Yb^{3+}:CaF2 and heavily doped Yb^{3+}:YLF as laser media at room temperature," *Optics Express*, vol. 17, no. 20, pp. 18312–18319, 2009.

[30] A. Pirri, D. Alderighi, G. Toci, and M. Vannini, "High-efficiency, high-power and low threshold Yb^{3+}:YAG ceramic laser," *Optics Express*, vol. 17, no. 25, pp. 23344–23349, 2009.

[31] J. Leitner, D. Sedmidubský, and P. Chuchvalec, "Prediction of heat capacities of solid binary oxides from group contribution method," *Ceramics-Silikáty*, vol. 46, no. 1, pp. 29–32, 2002.

[32] R. Peters, C. Kränkel, K. Petermann, and G. Huber, "Crystal growth by the heat exchanger method, spectroscopic characterization and laser operation of high-purity Yb:Lu_2O_3," *Journal of Crystal Growth*, vol. 310, no. 7–9, pp. 1934–1938, 2008.